
$\pi\gamma$ Transition FF in LCSRs and π DA: Global data fit

Alexander Bakulev, S. Mikhailov, A. Pimikov, and N. Stefanis
Bogoliubov Lab. Theor. Phys., JINR (Dubna, Russia)



PHIPSI'11
BINP, Novosibirsk

Outline:

- **Pion Distribution Amplitude (DA)**
- **Light-Cone Sum Rules (LCSRs) Approach**
- **LCSRs Results for $\pi\gamma$ Transition Form Factor (FF)**
- **Fitting Pion DA — Confidential Regions**
- **Confidential Region for Pion DA Moments vs. Lattice QCD**
- **Fit Results and Pion DA Models**
- **Conclusions**

Publications

Authors: A. B., S. Mikhailov, A. Pimikov, and N. Stefanis

Publications:

● A. B., S. M., N. S.	PLB	508	(2001)	279
● A. B., S. M., N. S.	PRD	67	(2003)	074012
● A. B., S. M., N. S.	PLB	578	(2004)	91
● A. B., S. M., N. S.	PRD	73	(2006)	056002
● A. B., A. P.	APPB	37	(2006)	3627
● A. B., A. P., N. S.	PRD	79	(2009)	093010
● S. M., N. S.	NPB	821	(2009)	291
● S. M., N. S.	MPLA	24	(2009)	2858
● A. B., S. M., N. S.	APPB	PS3	(2010)	943
● A. B., S. M., A. P., N. S.	PRD	84	(2011)	034014
● A. B., S. M., A. P., N. S.		arXiv:1108.4344		[hep-ph]
● N. S.		arXiv:1109.2718		[hep-ph]

Pion

Distribution Amplitude

(DA)

Pion distribution amplitude (DA)

- Matrix element of nonlocal axial current on light cone

$$\langle 0 | \bar{d}(z) \gamma_\mu \gamma_5 E(z, 0) u(0) | \pi(P) \rangle \Big|_{z^2=0} = \\ i f_\pi P_\mu \int_0^1 dx e^{ix(zP)} \varphi_\pi^{\text{TW-2}}(x, \mu^2)$$

- gauge-invariance due to Fock–Schwinger string:

$$E(z, 0) = \mathcal{P} e^{ig \int_0^z A_\mu(\tau) d\tau^\mu}$$

- Physical meaning of $\varphi_\pi(x; \mu^2)$ — amplitude for transition $\pi \rightarrow u + d$

Representation of Pion DA

- It is convenient to represent the pion DA:

$$\varphi_{\pi}(x; \mu^2) = \varphi^{\text{As}}(x) \times \left[1 + a_2(\mu^2) C_2^{3/2}(2x-1) + a_4(\mu^2) C_4^{3/2}(2x-1) + \dots \right]$$

where $C_n^{3/2}(2x-1)$ are the **Gegenbauer** polynomials (1-loop eigenfunctions of ER-BL kernel)

- That means

$$\{a_2(\mu^2), a_4(\mu^2), \dots\} \Leftrightarrow \varphi_{\pi}(x; \mu^2)$$

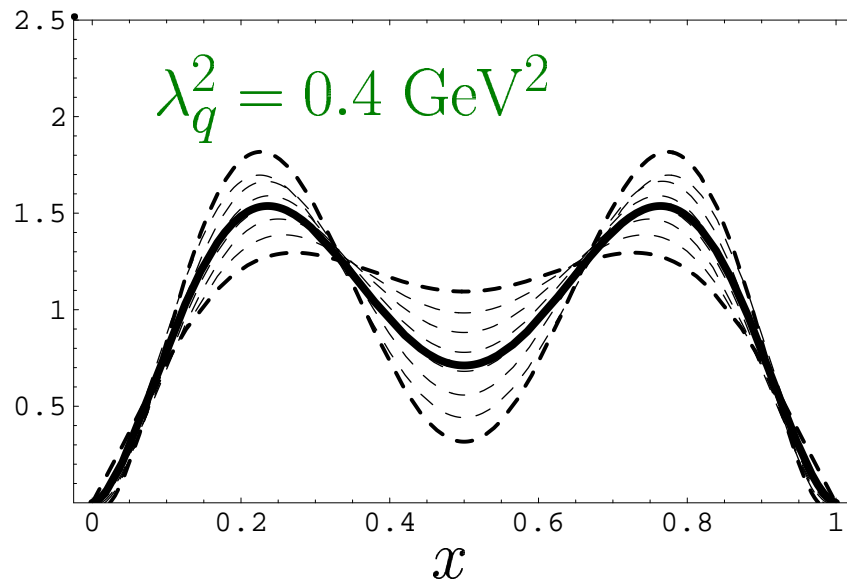
- ER-BL solution at 2-loop level

[Mikhailov&Radyushkin; 1986
Müller; 1994–95
A.B.&Stefanis; 2005]

NLC SRs for Pion DA

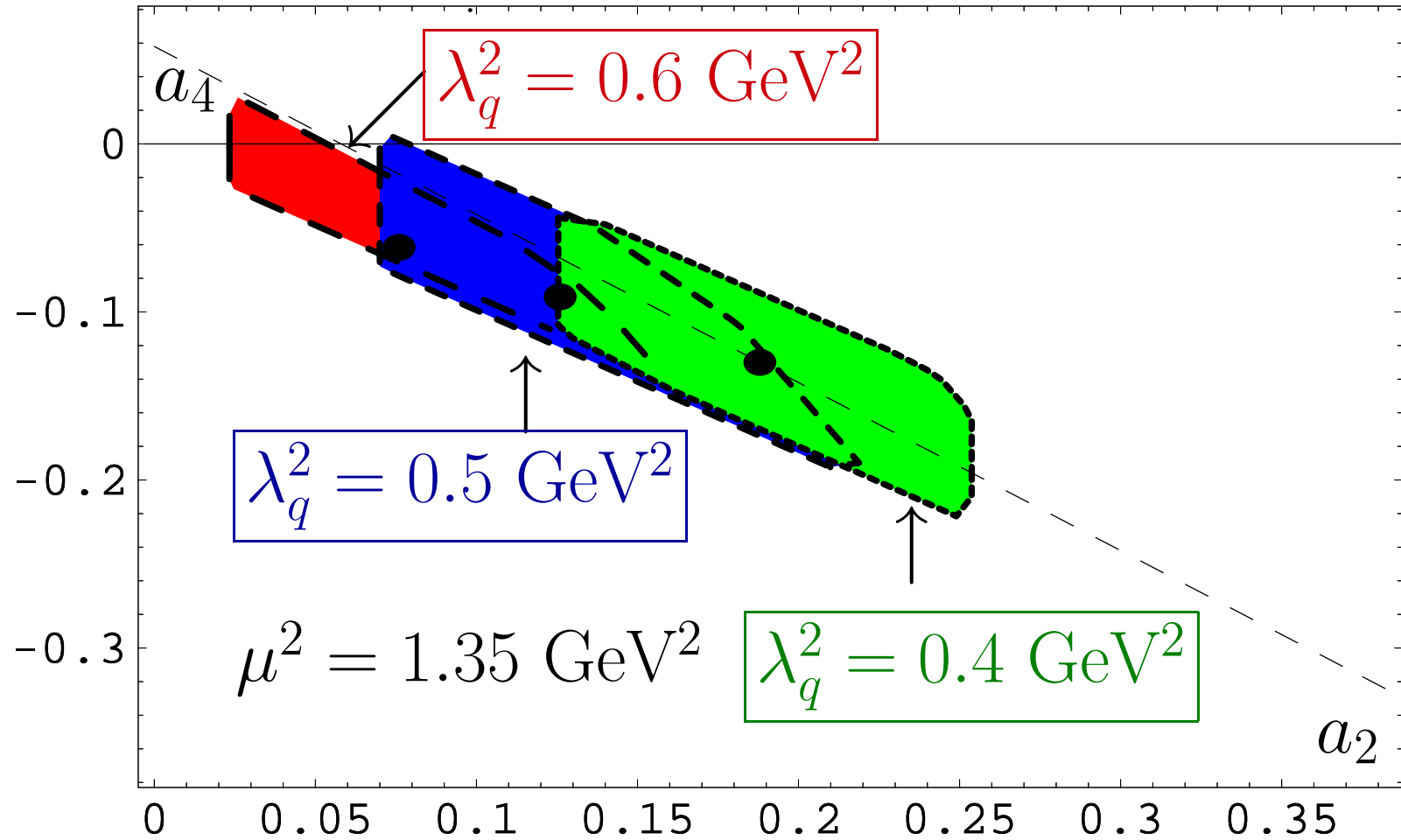
produce **bunch** of self-consistent 2-parameter models $\varphi_\pi(x)$
at $\mu^2 \simeq 1 \text{ GeV}^2$:

$$\varphi_\pi(x) = \varphi^{\text{As}}(x) \left[1 + a_2 C_2^{3/2}(2x-1) + a_4 C_4^{3/2}(2x-1) \right]$$



$a_2^{\text{b.f.}}$	=	+0.188
$a_4^{\text{b.f.}}$	=	-0.130
χ^2	\approx	0.001
$\langle x^{-1} \rangle^{\text{SR}}$	=	3.30(30)

NLC SR Constraints on a_2, a_4 of Pion DA



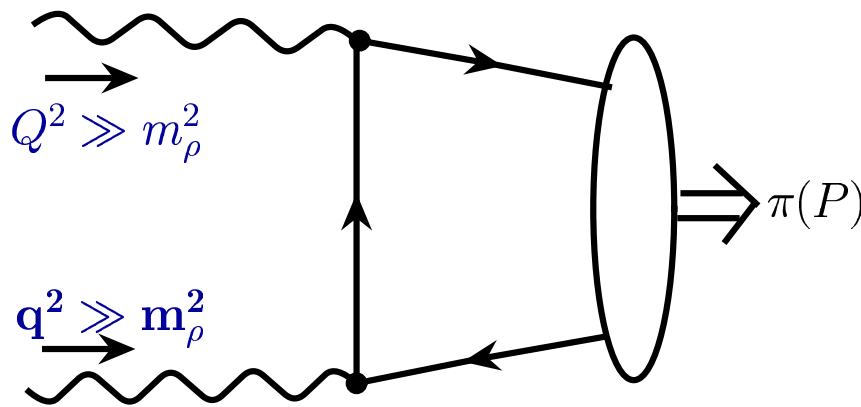
Estimated bunches of pion DAs for different values of λ_q^2 .

NLO Light-Cone SRs \Rightarrow
CLEO data on $F_{\gamma\gamma^*\pi}(Q^2) \Rightarrow$
Constraints on Pion DA

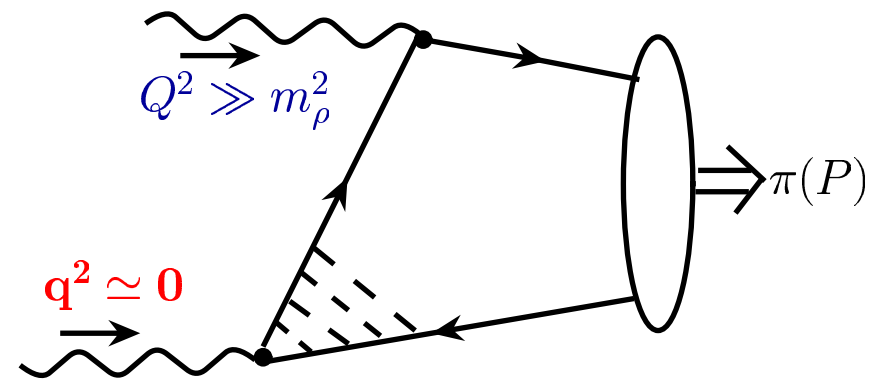
$\gamma^* \gamma \rightarrow \pi$: Why Light-Cone Sum Rules?

For $Q^2 \gg m_\rho^2$, $q^2 \ll m_\rho^2$ pQCD factorization valid only in leading twist and higher twists are of importance [Radyushkin–Ruskov, NPB (1996)].

Reason: if $q^2 \rightarrow 0$ one needs to take into account interaction of real photon at long distances $\sim O(1/\sqrt{q^2})$



pQCD is OK

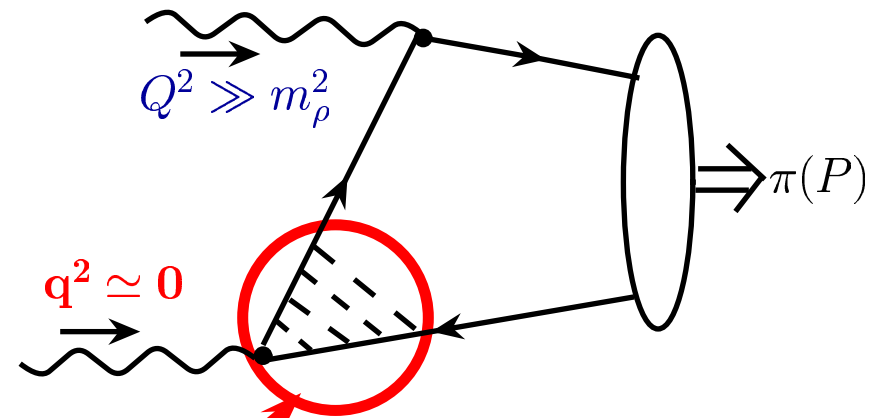


LCSRs should be applied

$\gamma^* \gamma \rightarrow \pi$: Why Light-Cone Sum Rules?

For $Q^2 \gg m_\rho^2$, $q^2 \ll m_\rho^2$ pQCD factorization valid only in leading twist and higher twists are of importance [Radyushkin–Ruskov, NPB (1996)].

Reason: if $q^2 \rightarrow 0$ one needs to take into account interaction of real photon at long distances $\sim O(1/\sqrt{q^2})$



To account for long-distance effects in pQCD one needs to introduce light-cone **DA** of real photon

$\gamma^* \gamma \rightarrow \pi$: *Light-Cone Sum Rules!*

Khodjamirian [EJPC (1999)]: LCSR effectively accounts for long-distances effects of real photon using quark-hadron duality in vector channel and dispersion relation in q^2

$$F_{\gamma\gamma^*\pi}(Q^2, q^2) = \frac{1}{\pi} \int_0^{s_0} \frac{\text{Im}F_{\gamma^*\gamma^*\pi}^{\text{PT}}(Q^2, s)}{m_\rho^2 + q^2} e^{(m_\rho^2 - s)/M^2} ds + \frac{1}{\pi} \int_{s_0}^{\infty} \frac{\text{Im}F_{\gamma^*\gamma^*\pi}^{\text{PT}}(Q^2, s)}{s + q^2} ds$$

$s_0 \simeq 1.5 \text{ GeV}^2$ – effective threshold in vector channel,
 M^2 – Borel parameter (0.5 – 0.9 GeV^2).

Real-photon limit $q^2 \rightarrow 0$ can be easily done ...

$\gamma^* \gamma \rightarrow \pi$: *Light-Cone Sum Rules!*

Khodjamirian [EJPC (1999)]: LCSR effectively accounts for long-distances effects of real photon using quark-hadron duality in vector channel and dispersion relation in q^2

$$F_{\gamma\gamma^*\pi}(Q^2, 0) = \frac{1}{\pi} \int_0^{s_0} \frac{\text{Im}F_{\gamma^*\gamma^*\pi}^{\text{PT}}(Q^2, s)}{m_\rho^2} e^{(m_\rho^2 - s)/M^2} ds + \frac{1}{\pi} \int_{s_0}^{\infty} \frac{\text{Im}F_{\gamma^*\gamma^*\pi}^{\text{PT}}(Q^2, s)}{s} ds$$

$s_0 \simeq 1.5 \text{ GeV}^2$ – effective threshold in vector channel,
 M^2 – Borel parameter (0.5 – 0.9 GeV^2).

... as demonstrated here.

Main Ingredients of Spectral Density

We denote

$$\rho(Q^2, s) = \rho^{(0)}(Q^2, s) + a_s \rho^{(1)}(Q^2, s) + a_s^2 \rho^{(2)}(Q^2, s)$$

- **NLO Spectral Density** — in [Mikhailov&Stefanis(2009)], partially corrected in [ABOP(2011)]:

$$\rho^{(1)}(Q^2, s) = \frac{\text{Im}}{\pi} [(T_1 \otimes \varphi_\pi)(Q^2, -s - i\varepsilon)] , s \geq 0$$

- **NNLO_{β₀} Spectral Density** — in [M&S(2009)]

$$\rho^{(2,\beta)}(Q^2, s) = \beta_0 \frac{\text{Im}}{\pi} [(T_{2\beta} \otimes \varphi_\pi)(Q^2, -s - i\varepsilon)] , s \geq 0$$

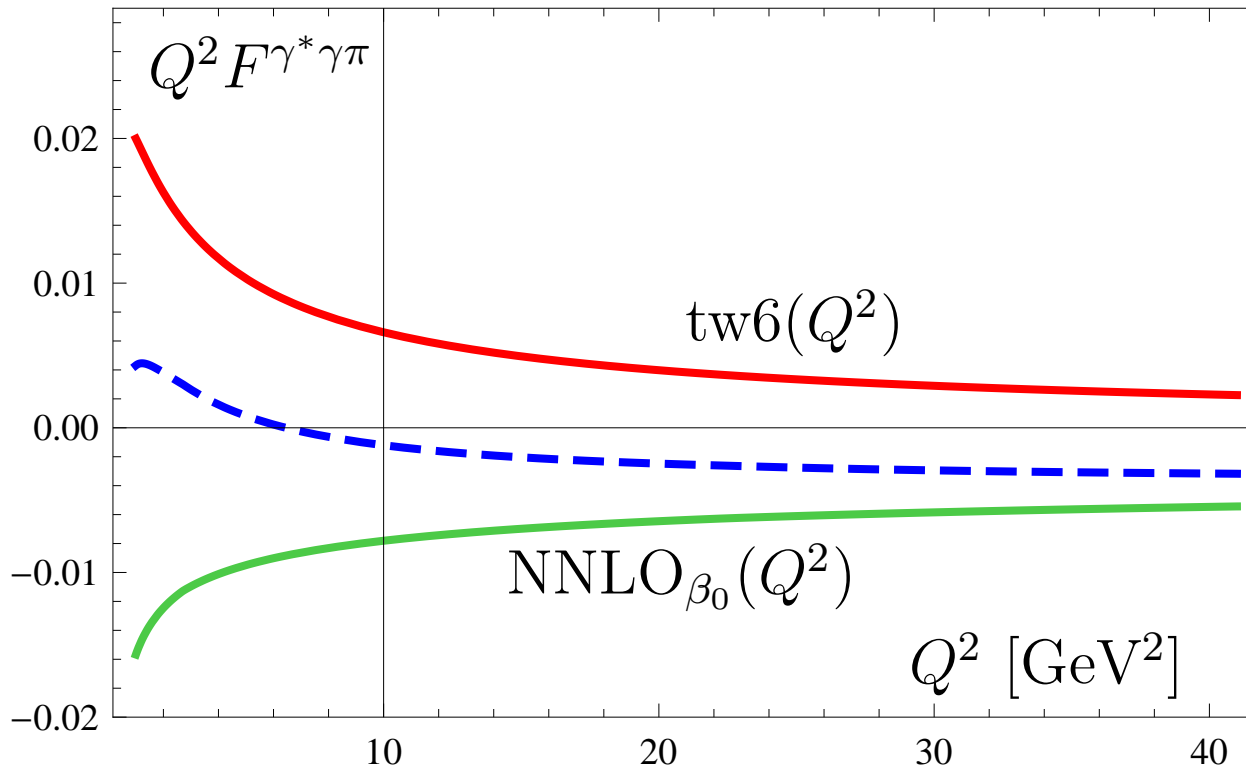
Both $\rho^{(1)}$ and $\rho^{(2,\beta)}$ are obtained for arbitrary Gegenbauer harmonic.

- “Tw-6” contribution — in [ABOP-PRD83(2011)0540020]

$$\rho^{\text{tw}6}(Q^2, x) = 8\pi C_F \frac{\alpha_s \langle \bar{q}q \rangle^2}{N_c f_\pi^2} \frac{x^2}{Q^6} \left[2x \ln x \bar{x} - x + 2\delta(\bar{x}) - \left[\frac{1}{1-x} \right]_+ \right]$$

High order corrections result

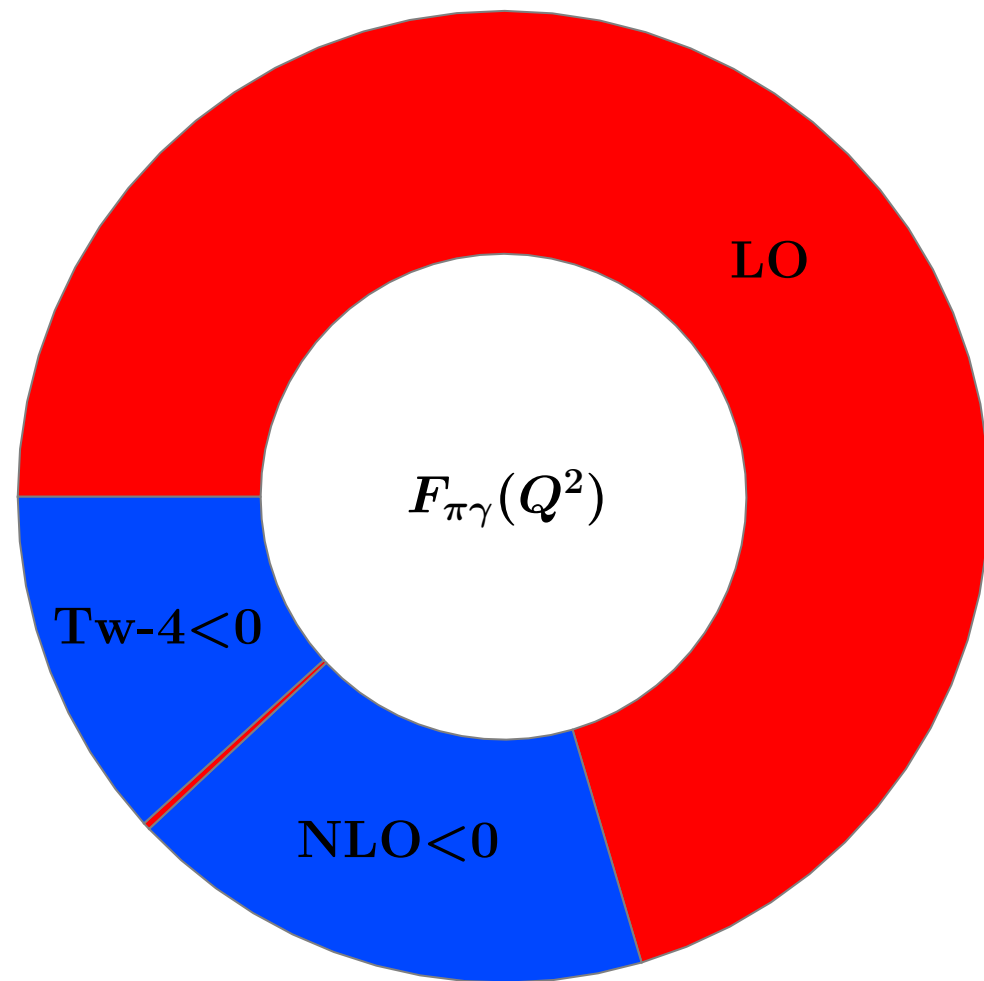
Twist-6 and **NNLO $_{\beta_0}$** contributions to the $Q^2 F^{\gamma^* \gamma \pi}(Q^2)$
with **BMS-like Pion DA**
They practically cancel out each other [BMPS(2011)]



We use this residual as **theoretical uncertainty** of our prediction, that provides us with an additional **3%-uncertainty**.

Pie chart for Pion-Photon TFF at $Q^2 = 8 \text{ GeV}^2$

- Result is dominated by Hard Part of Twist-2 LO contribution.

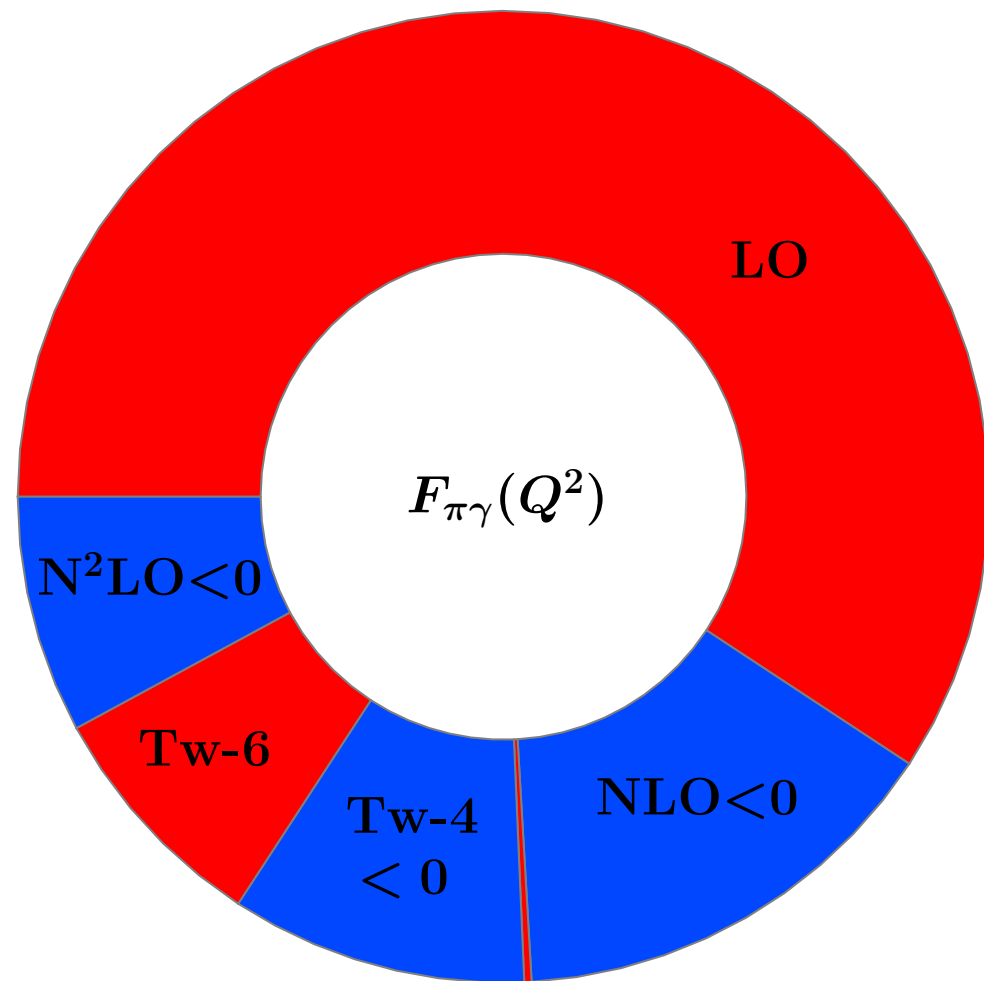


Blue = negative terms

Red = positive terms

Pie chart for Pion-Photon TFF at $Q^2 = 8 \text{ GeV}^2$

- Result is dominated by Hard Part of Twist-2 LO contribution.
- **Twist-6 contribution** is taken into account together with **NNLO $_{\beta_0}$ one** — they have close absolute values and opposite signs.



Blue = negative terms

Red = positive terms

Parameters of LCSRs

From PDG:

- $\alpha_s(m_Z^2)$
- Masses m_ρ, m_ω
- Decay Widths $\Gamma_\rho, \Gamma_\omega$

From QCD SR:

- Borel parameter $M_{\text{LC SR}}^2$
- Vector Chan. Threshold s_0
- Twist-4 $\delta^2 \pm 20\%$
- Twist-6 ($\alpha_s \langle \bar{q}q \rangle$)

Light-Cone Sum Rules:

$$\text{LO} + \text{NLO} + \text{Tw-4} + (\text{NNLO}_{\beta_0} + \text{Tw-6})$$

π -DA model

Data on FF

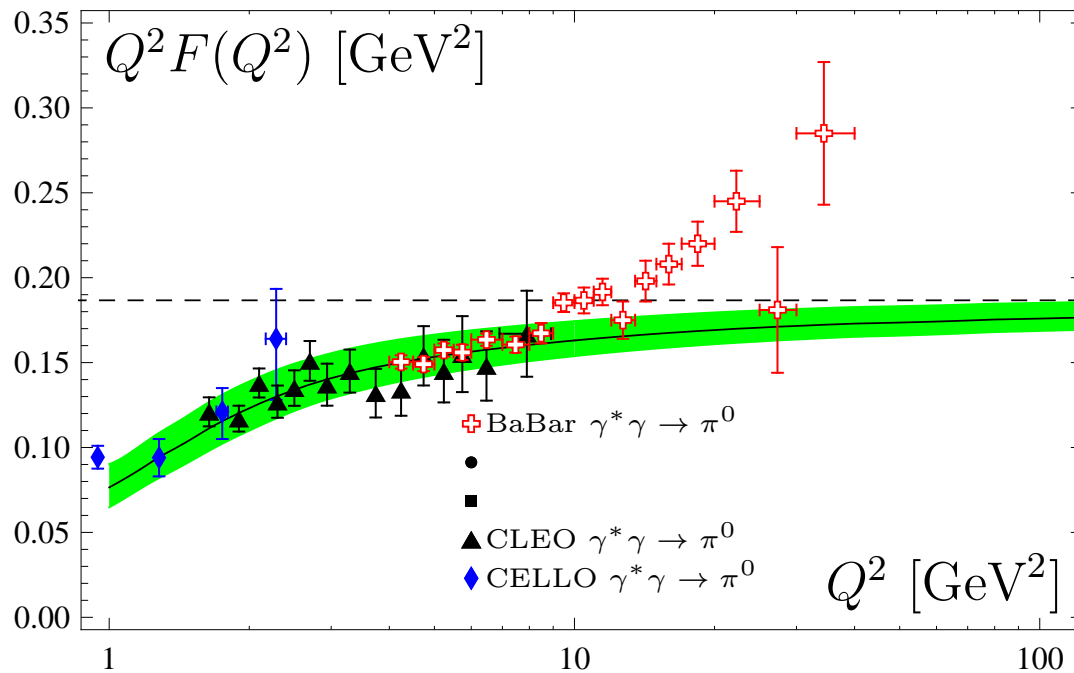
FF Prediction

Fitting π -DA (a_n)

LCSRs Results for Pion-Gamma Transition FF

Pion-gamma FF vs Experimental Data

Comparison with all data: CELLO, CLEO and BaBar

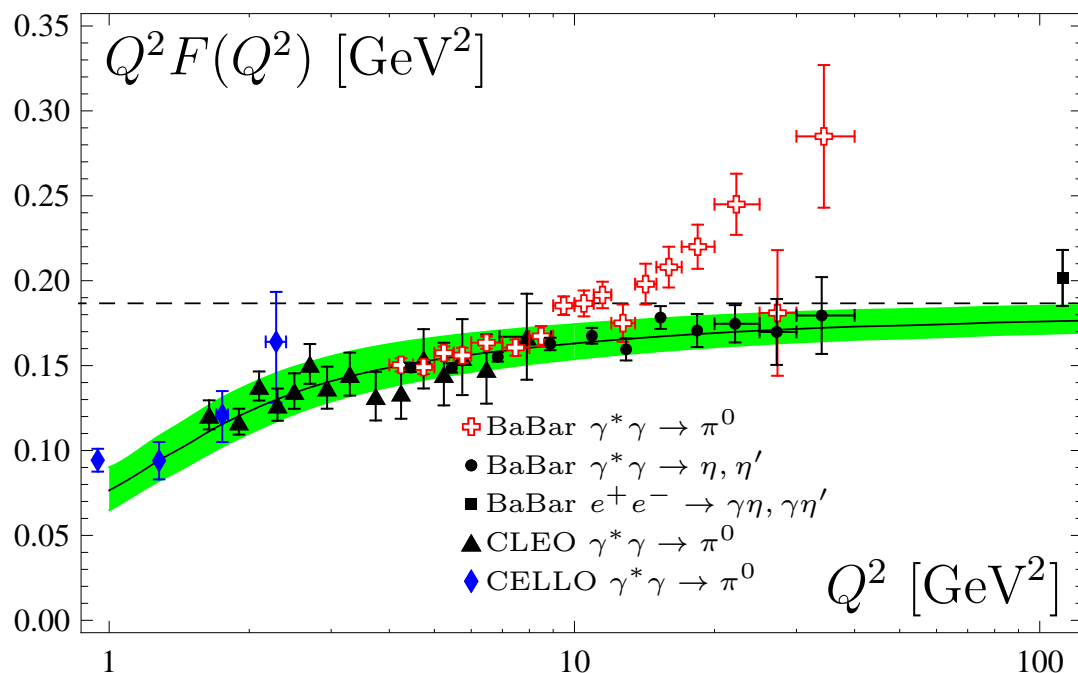


curve	DA
-----	Asymp.QCD
	BMS bunch

● **BMS bunch** describes very good all data for $Q^2 \leq 9 \text{ GeV}^2$.

Pion-gamma FF vs Experimental Data

Comparison with all data: CELLO, CLEO and BaBar



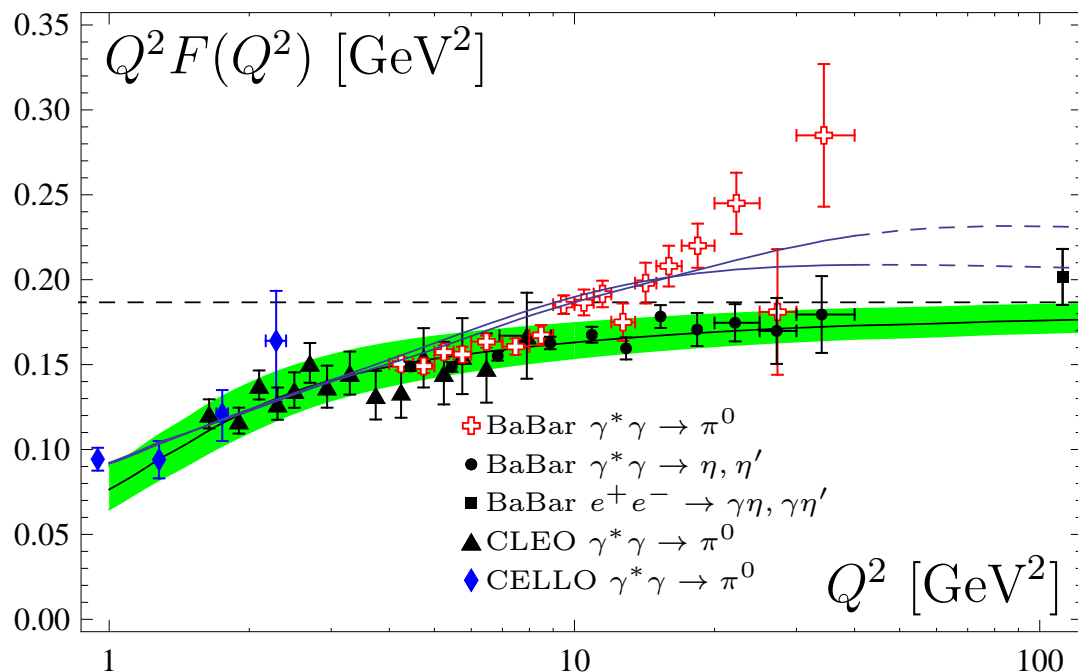
curve	DA
-----	Asymp.QCD
	BMS bunch



● **BMS bunch** describes very good all data for $Q^2 \leq 9 \text{ GeV}^2$.

● Note added BaBar $\gamma^* \gamma \rightarrow \eta, \eta'$ and $e^+ e^- \rightarrow \gamma \eta, \gamma \eta'$ data (1101.1142[hep-ex]): All they are inside **BMS strip** !

Pion-gamma FF vs Experimental Data

Comparison with all data: CELLO, CLEO and BaBar



curve	DA
-----	Asymp.QCD
	BMS bunch
	ABOP-1,3
Agaev et al	PRD83-054020

- BMS bunch describes very good all data for $Q^2 \leq 9 \text{ GeV}^2$.
- Note added BaBar $\gamma^* \gamma \rightarrow \eta, \eta'$ and $e^+ e^- \rightarrow \gamma \eta, \gamma \eta'$ data (1101.1142[hep-ex]): All they are inside BMS strip !
- ABOP models are in between two sets of BaBar data.

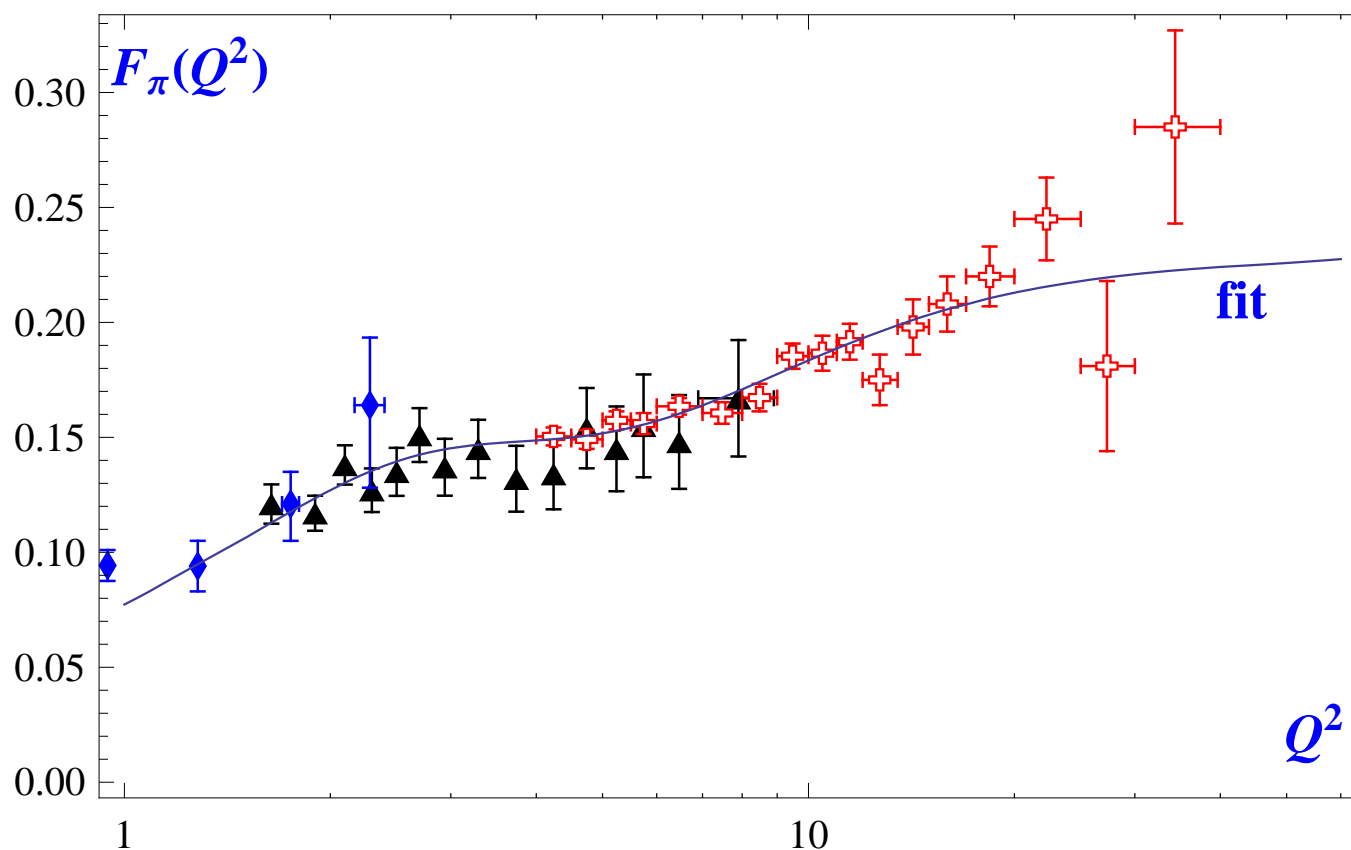
Fitting Pion DA

—

Confidential Regions

Fitting pion DA under LCSR

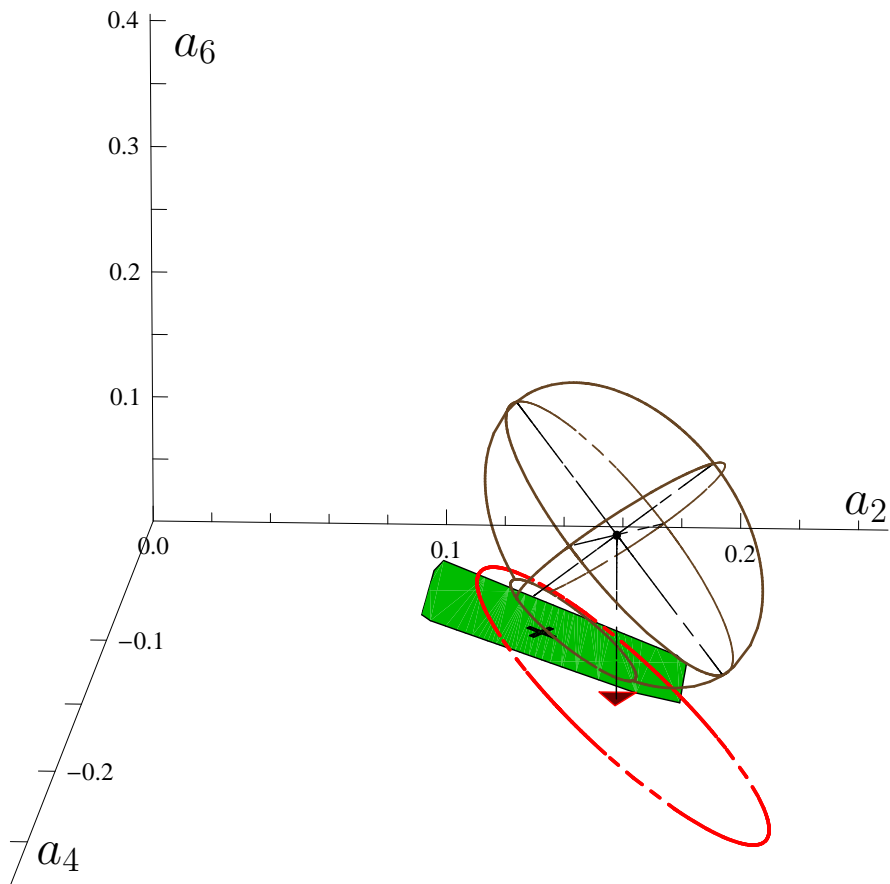
- We fitted experimental data on $\pi\gamma$ TFF by varying Gegenbauer coefficients of Pion DA.
- Two sets of experim. data ($1 - 9 \text{ GeV}^2$ & $1 - 40 \text{ GeV}^2$) were analyzed to show the influence of BaBar Data on Pion DA.



Fit based on LCSRs with NLO+Tw4+3 Gegenbauers

NLC SR Results vs 3D Constraints

BMPS [PRD84(2011)034014]: 3D 1σ -error ellipsoid at $\mu_{SY} = 2.4$ GeV scale without $\Delta\delta_{tw4}^2$ uncertainty



Data Set 1 – 9 GeV²

— \Leftrightarrow **2D projection of 1σ -error ellipsoid**

▼ \Leftrightarrow **$\chi_{ndf}^2 \approx 0.4$**

✕ \Leftrightarrow **BMS model with $\chi_{ndf}^2 \approx 0.5$**

Best-fit = (0.17, -0.14, 0.12 \pm 0.14)

BMS = (0.14, -0.09)

Good agreement of all data at $Q^2 \leq 9$ GeV²

At 68.3% CL we have good intersection $2D \cap 3D \cap 4D \neq \emptyset$

NLC SR Results vs 3D Constraints

BMPS [PRD84(2011)034014]: 3D 1σ -error ellipsoid at $\mu_{SY} = 2.4$ GeV scale without $\Delta\delta_{tw4}^2$ uncertainty



Data Set 1 – 9 GeV²

— \Leftrightarrow 2D projection of 1σ -error ellipsoid

▼ $\Leftrightarrow \chi_{\text{ndf}}^2 \approx 0.4$

✕ \Leftrightarrow BMS model with $\chi_{\text{ndf}}^2 \approx 0.5$

Best-fit = $(0.17, -0.14, 0.12 \pm 0.14)$

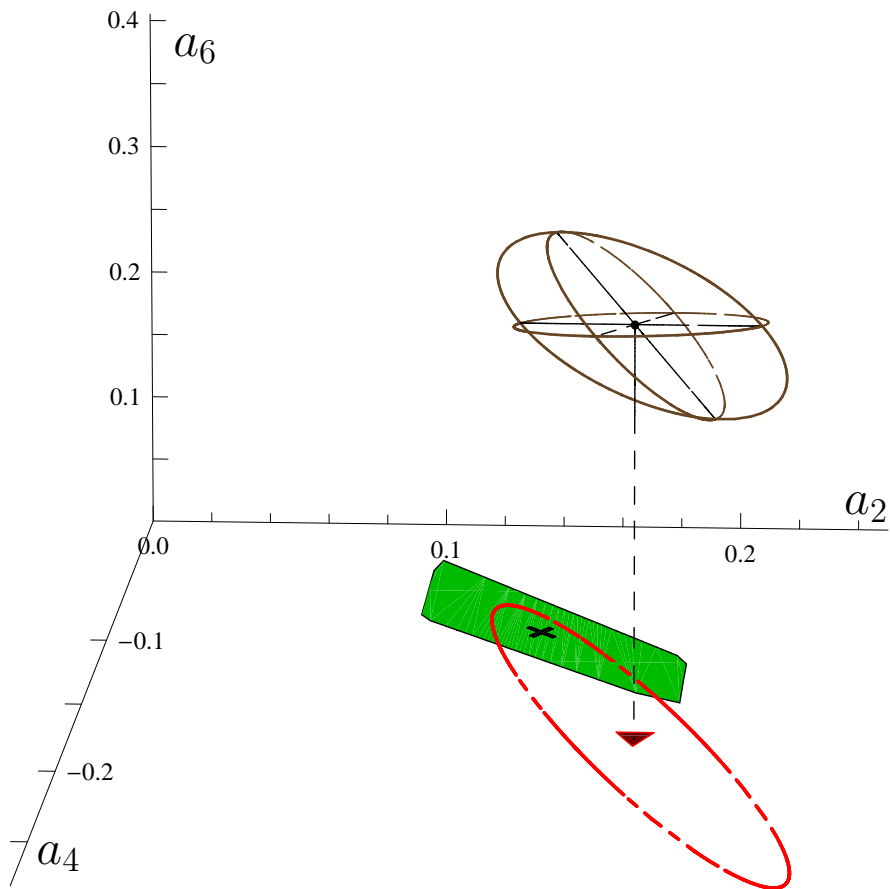
BMS = $(0.14, -0.09)$

Good agreement of all data at $Q^2 \leq 9$ GeV²

At 68.3% CL we have good intersection $2D \cap 3D \cap 4D \neq \emptyset$

NLC SR Results vs 3D Constraints

BMPS [PRD84(2011)034014]: 3D 1σ -error ellipsoid at $\mu_{SY} = 2.4$ GeV scale without $\Delta\delta_{tw4}^2$ uncertainty



Data Set 1 – 40 GeV²

— \Leftrightarrow **2D projection of 1σ -error ellipsoid**

▼ \Leftrightarrow **$\chi_{ndf}^2 \approx 1.0$**

✕ \Leftrightarrow **BMS model with $\chi_{ndf}^2 \approx 3.1$**

Best-fit = (0.18, -0.17, 0.31 \pm 0.1)

BMS = (0.14, -0.09)

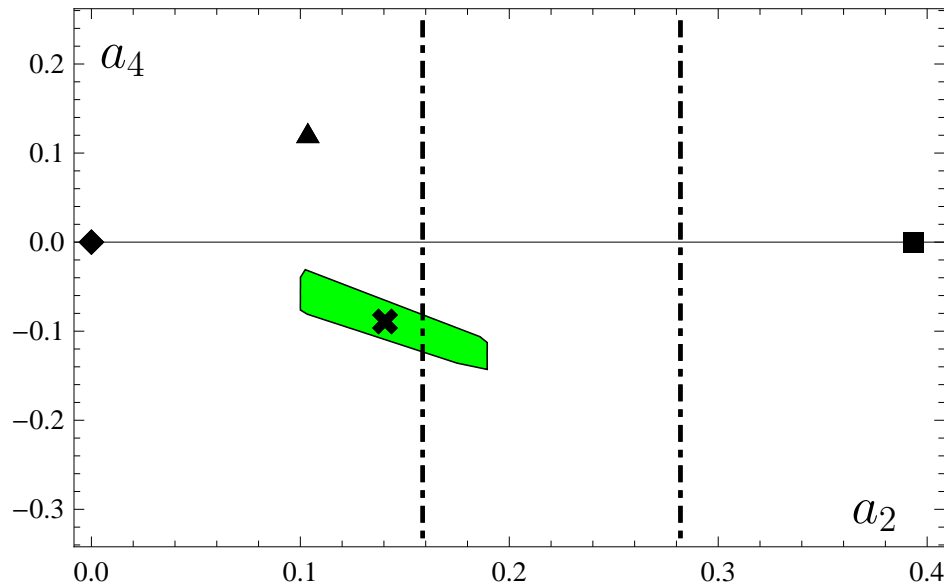
Bad agreement of all data at $Q^2 \leq 40$ GeV²

At 68.3% CL we have no intersection $2D \cap 3D = \emptyset$, $3D \cap 4D = \emptyset$.

NLC SR Results vs 2D Constraints

NLC-bunch and lattice prediction at $\mu_{SY} = 2.4$ GeV scale with accounting for $\Delta\delta_{tw4}^2$ uncertainty.

DAs: $\blacklozenge \Leftrightarrow$ Asymp., $\blacktriangle \Leftrightarrow$ ABOP-3, $\blacktimes \Leftrightarrow$ BMS, $\blacksquare \Leftrightarrow$ CZ
Lattice'10 estimate of a_2 are shown by vertical lines.



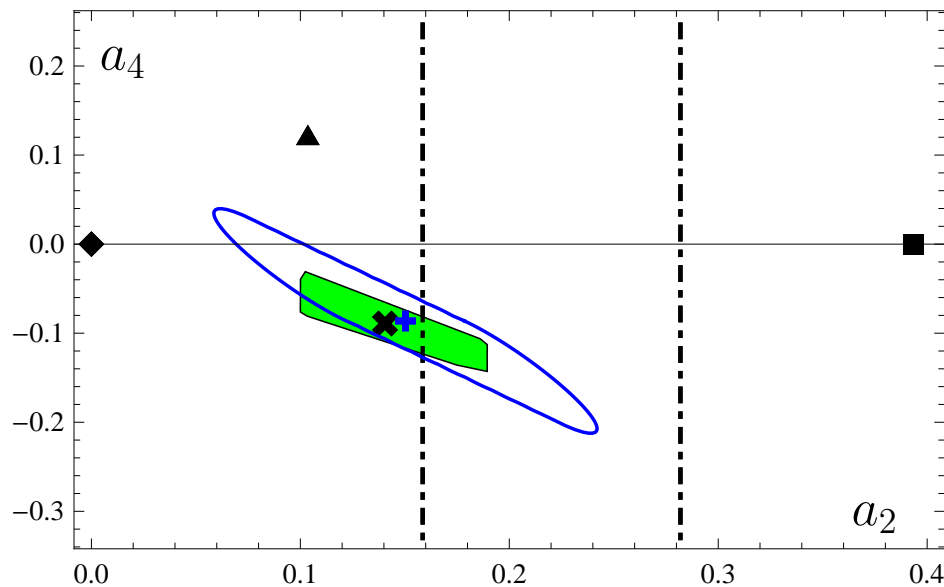
Data Set 1 – 9 GeV²

BMS bunch agrees well with the lattice data

NLC SR Results vs 2D Constraints

2D-Analysis of the data at $\mu_{\text{SY}} = 2.4$ GeV scale
with accounting for $\Delta\delta_{\text{tw}4}^2$ uncertainty.

DAs: $\blacklozenge \Leftrightarrow$ Asymp., $\blacktriangle \Leftrightarrow$ ABOP-3, $\blacktimes \Leftrightarrow$ BMS, $\blacksquare \Leftrightarrow$ CZ
Lattice'10 estimate of a_2 are shown by vertical lines.



Data Set 1 – 9 GeV²

— \Leftrightarrow 2D 1σ -error ellipse

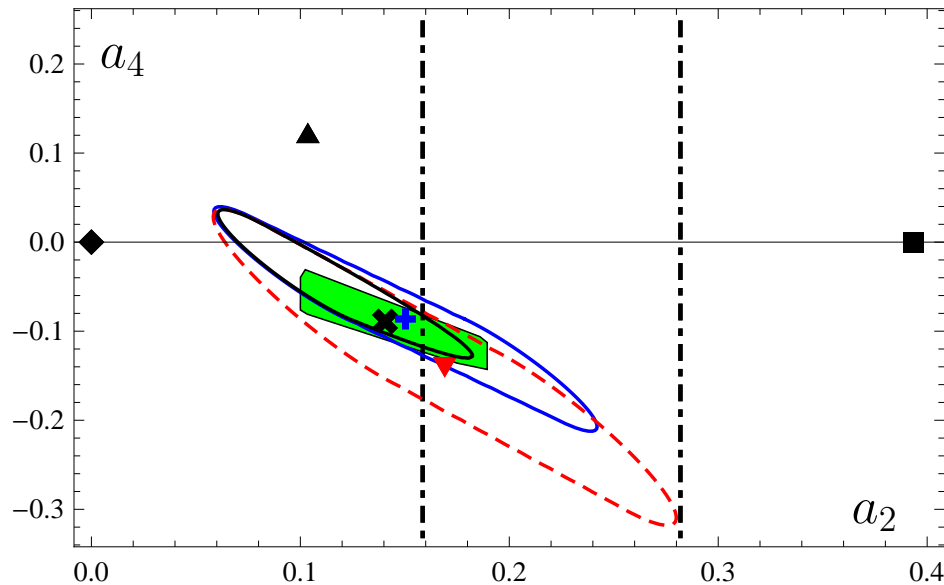
BMS bunch agrees well with the lattice data

BMS bunch has better agreement with data up 9 GeV² than with CLEO data only.

NLC SR Results vs 2D Constraints

2D-Analysis of the data at $\mu_{\text{SY}} = 2.4$ GeV scale
with accounting for $\Delta\delta_{\text{tw}4}^2$ uncertainty.

DAs: $\blacklozenge \Leftrightarrow$ Asymp., $\blacktriangle \Leftrightarrow$ ABOP-3, $\times \Leftrightarrow$ BMS, $\blacksquare \Leftrightarrow$ CZ
Lattice'10 estimate of a_2 are shown by vertical lines.



Data Set 1 – 9 GeV²

- — \Leftrightarrow 2D 1 σ -error ellipse
- --- \Leftrightarrow 2D-Proj. 3D-ellipsoid
- — \Leftrightarrow $a_6 = 0$ cut of 3D-ellipsoid

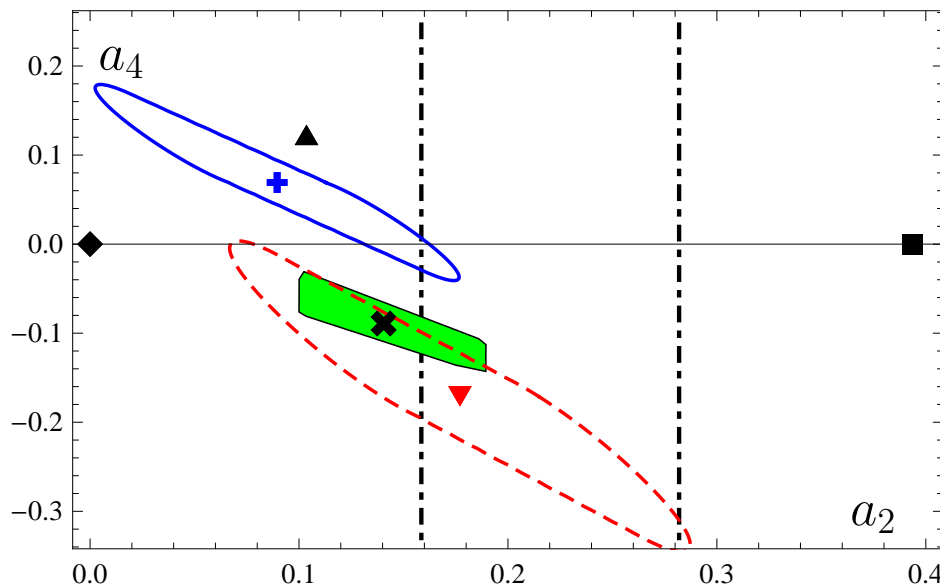
BMS bunch agrees well with the lattice data

BMS bunch has better agreement with data up 9 GeV² than
with CLEO data only.

NLC SR Results vs 2D Constraints

BMPS [arXiv:1105.2753 [hep-ph]]: 2D 1σ -error ellipses at $\mu_{SY} = 2.4$ GeV scale with accounting for $\Delta\delta_{tw4}^2$ uncertainty.

DAs: $\blacklozenge \Leftrightarrow$ Asymp., $\blacktriangle \Leftrightarrow$ ABOP-3, $\blacktimes \Leftrightarrow$ BMS, $\blacksquare \Leftrightarrow$ CZ
Lattice'10 estimate of a_2 are shown by vertical lines.



Data Set 1 – 40 GeV²

— \Leftrightarrow 2D 1σ -error ellipse

- - - \Leftrightarrow 2D-Proj. 3D-ellipsoid

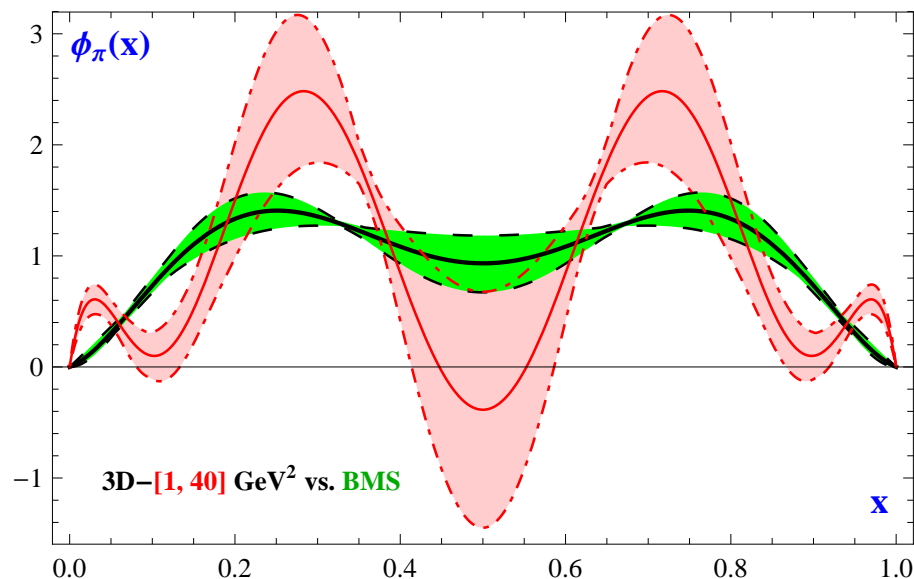
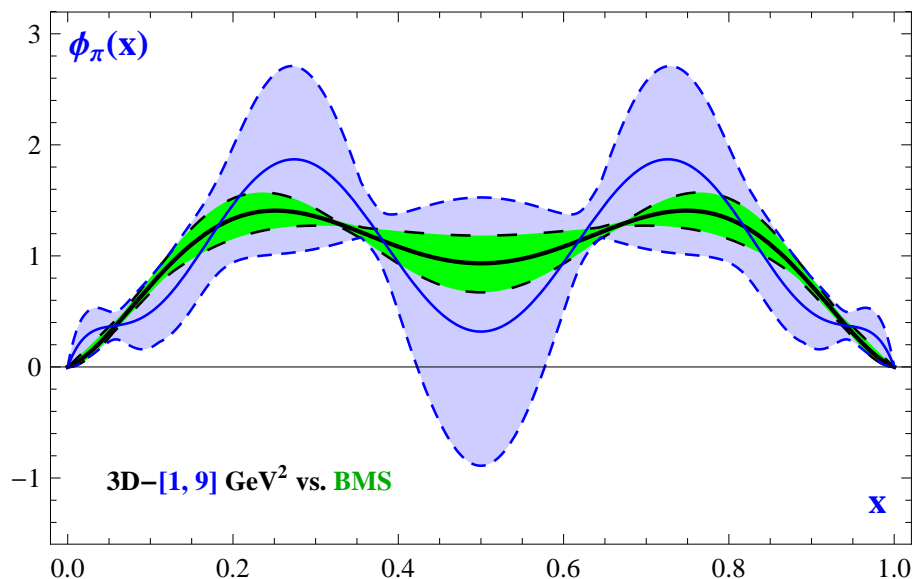
Bad agreement with 2D 1σ -error ellipse

No cross-section with $a_6 = 0$ plane.

3D Data Fit of Pion DA vs BMS (QCD SR)

■ := BMS, **■** := $1 - 9 \text{ GeV}^2$, **■** := $1 - 40 \text{ GeV}^2$

at $\mu_{\text{SY}} = 2.4 \text{ GeV}$ scale.



- BMS bunch agrees well with Data Set $1 - 9 \text{ GeV}^2$;
- New BaBar Data do not agree with BMS bunch based on NLC QCD SRs.
- Both data sets does not match each other.

End-point Behavior of Pion DA

Integral derivative $D^{(2)}\varphi(x) = \frac{1}{x} \int_0^x \frac{\varphi(y)}{y} dy$

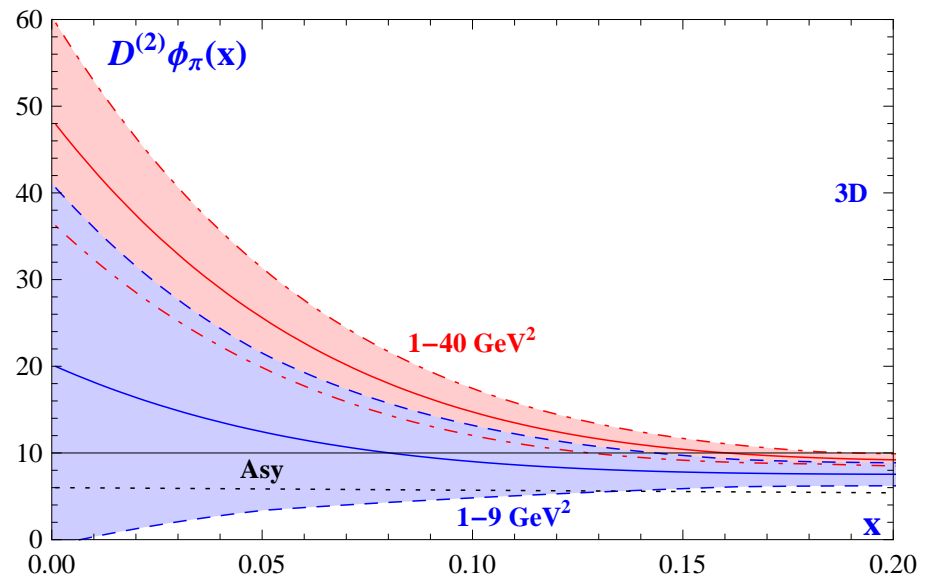
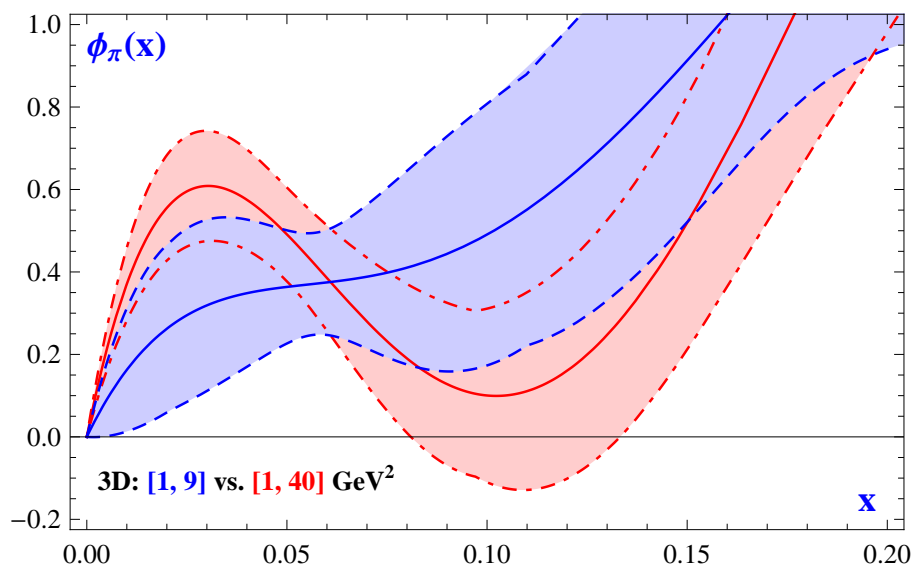
is an average derivative $\varphi'_\pi(x)$ near the end-point $x = 0$.

Important property: $\lim_{x \rightarrow 0} D^{(2)}\varphi(x) = \varphi'_\pi(0)$.

End-point Behavior of Pion DA

$$\text{Integral derivative } D^{(2)}\varphi(x) = \frac{1}{x} \int_0^x \frac{\varphi(y)}{y} dy$$

at $\mu_{\text{SY}} = 2.4 \text{ GeV}$ scale.





● $DA^{1-9 \text{ GeV}^2}$ and $DA^{1-40 \text{ GeV}^2}$ are separated near the origin.

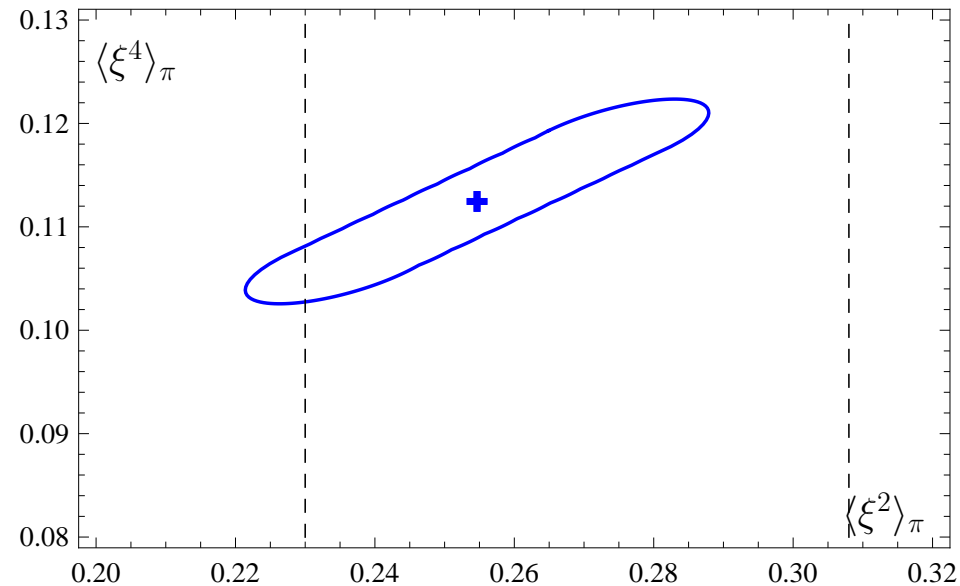
● **BaBar Data** demands End-Point Enhanced Pion DA.

Confidential Region for Pion DA Moments vs. Lattice QCD

2D Constraints and Lattice QCD

1σ region in $(\langle\xi^2\rangle_\pi, \langle\xi^4\rangle_\pi)$ plane from $2D(1 - 9 \text{ GeV}^2)$ analysis vs QCDSF&UKQCD Lattice Data [PRD74(2006)074501] at $\mu_{\text{lat}} = 2 \text{ GeV}$ scale:




curve	meaning
	2D-1σ-ellipse
	Lattice'06

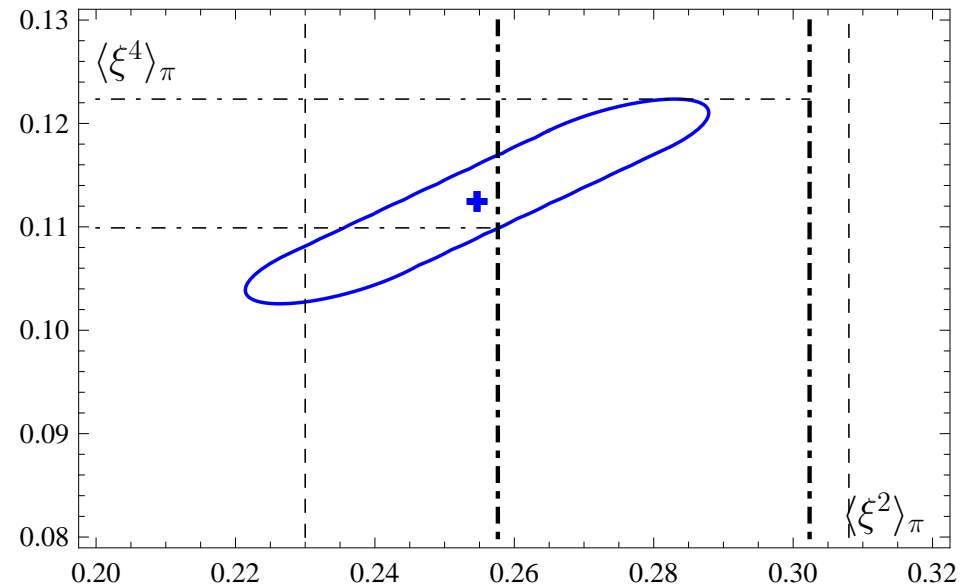


Our **2D- 1σ** region is almost completely inside **Lattice'06** constraint.

2D Constraints and Lattice QCD

1σ region in $(\langle\xi^2\rangle_\pi, \langle\xi^4\rangle_\pi)$ plane from **2D(1 – 9 GeV²)** analysis vs **RBC&UKQCD Lattice Data [PRD83(2011)074505]** at $\mu_{\text{lat}} = 2$ GeV scale:





curve	meaning
	2D-1σ-ellipse
	Lattice'06
	Lattice'10

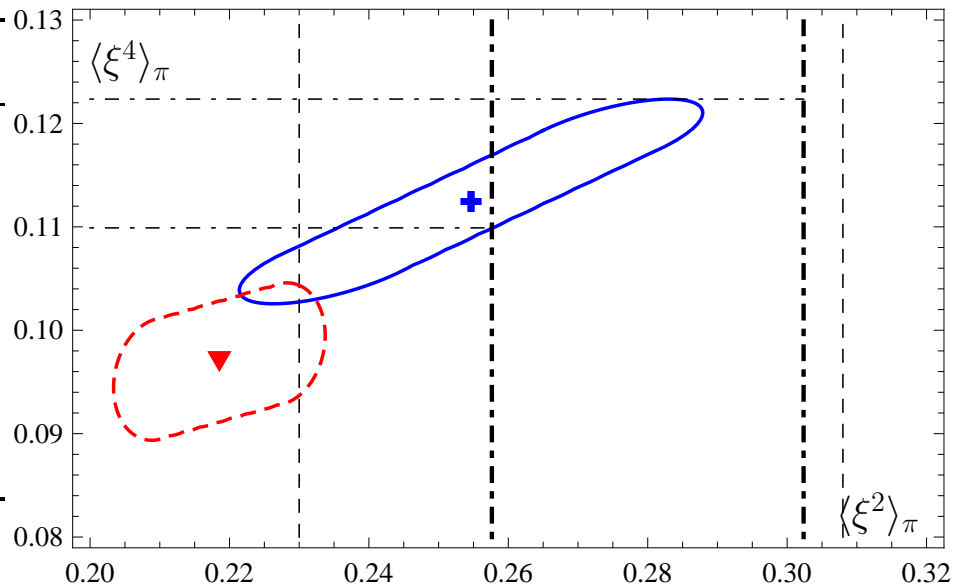


Our **2D-1 σ** region is one-half inside **Lattice'10** constraint.

2D Constraints and Lattice QCD

1σ region in $(\langle\xi^2\rangle_\pi, \langle\xi^4\rangle_\pi)$ plane from $2D(1 - 9 \text{ GeV}^2)$ analysis vs RBC&UKQCD Lattice Data [PRD83(2011)074505] at $\mu_{\text{lat}} = 2 \text{ GeV}$ scale:

curve	meaning
	$2D^{0.7}$ - 1σ -ellipse
	Lattice'06
	Lattice'10
	$2D^{1.5}$ - 1σ -ellipse






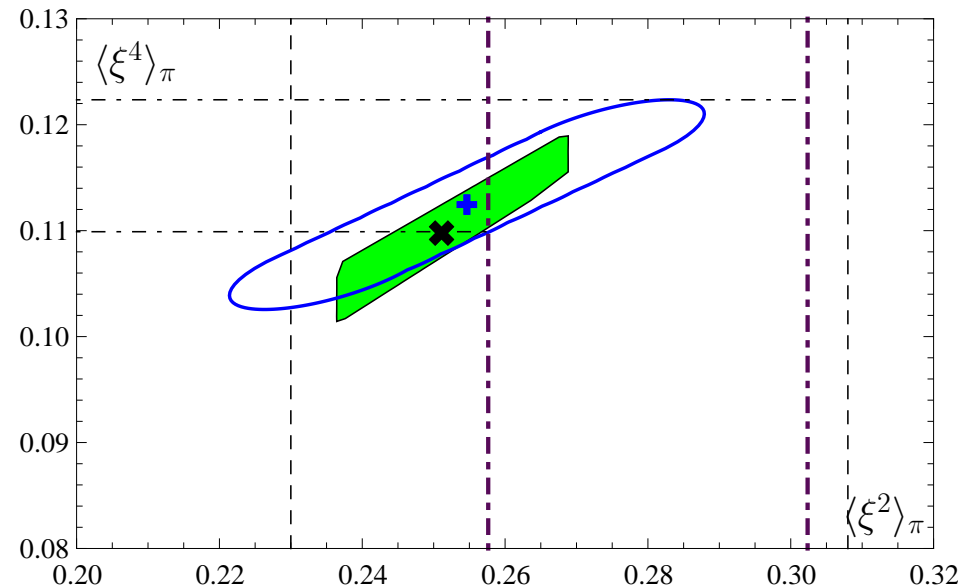
Our $2D$ - 1σ region with $(M^2 \approx 0.7 \text{ GeV}^2)$ is one-half inside Lattice'10 constraint,

whereas the $2D$ - 1σ region with ABOP value $(M^2 = 1.5 \text{ GeV}^2)$ is completely out of Lattice'10 constraint!

2D Constraints and Lattice QCD

1σ region in $(\langle\xi^2\rangle_\pi, \langle\xi^4\rangle_\pi)$ plane from **2D(1 – 9 GeV²)** analysis
vs **RBC&UKQCD Lattice Data [PRD83(2011)074505]** at
 $\mu_{\text{lat}} = 2$ GeV scale:

curve	meaning
	2D-1σ-ellipse
	Lattice'06
	Lattice'10



Intersection of Lattice and **2D-1 σ** region leads to prediction:

$\langle\xi^4\rangle_\pi \in [0.11, 0.122]$ — in a good agreement with estimation
 $\langle\xi^4\rangle_\pi \in [0.095, 0.134]$ in **[Stefanis, NPB.PS.181(2008)199]**.

Fit Results and Pion DA Models

Comparing Fit Results with Pion DA models

Model/Fit	Values of a_n	χ^2/ndf (1 – 9 GeV ²)	χ^2/ndf (1 – 40 GeV ²)
a_2, a_4, a_6 Fit	(0.18, -0.17, 0.31)	0.4	1.0
BMS	(0.14, -0.09)	0.5	3.1
Agaev et al	(0.08, 0.14, 0.09)	2.8	2.4
Kroll	(0.21, 0.01)	3.8	4.4
AdS/QCD	0.15, 0.06, 0.03	2.3	2.8
CZ	(0.39)	32.3	25.5
Asympt.	(0, 0)	4.7	7.9

All values given at $\mu_{\text{SY}} = 2.4$ GeV scale.

- **BMS DA** gives best LCSR Description of $\pi\gamma$ TFF for $Q^2 \leq 9 \text{ GeV}^2$.
- All-Data LCSR-Fit Result is far from All Considered **Pion DA Models**.

Comparing Different Data Set Analyses

Q^2 regions	[1 – 9] GeV^2	[1 – 40] GeV^2
BMS bunch	Agreement	No!
η and η'	Agreement	No!
Number of harmonics n	2, 3	3, 4
Best χ_{ndf}^2	0.53, 0.44	1.0, 0.77
Derivative $\varphi_\pi(x) _{x=0}$	$20.2 \pm 19.8 \pm 1.1$	$48.5 \pm 11.4 \pm 0.4$
Derivative $D^{(2)}\varphi_\pi(0.4)$	$6.6 \pm 1.1 \pm 0.4$	$8.1 \pm 0.7 \pm 0.3$

Conclusions

- By fitting $\pi\gamma$ Transition FF Data in LCSR Approach we obtained Confidential Regions for Gegenbauer coefficients, Moments, and Derivatives of Pion DA.

Conclusions

- By fitting $\pi\gamma$ Transition FF Data in LCSR Approach we obtained Confidential Regions for Gegenbauer coefficients, Moments, and Derivatives of Pion DA.
- Result of fitting the CELLO, CLEO, and BaBar Data up to 9 GeV^2 is in a good agreement with previous CLEO-based fit and prefers the End-Point Suppressed (BMS) Pion DA.

Conclusions

- By fitting $\pi\gamma$ Transition FF Data in LCSR Approach we obtained Confidential Regions for Gegenbauer coefficients, Moments, and Derivatives of Pion DA.
- Result of fitting the CELLO, CLEO, and BaBar Data up to 9 GeV^2 is in a good agreement with previous CLEO-based fit and prefers the End-Point Suppressed (BMS) Pion DA.
- Taking into account all the data on $F_{\gamma^*\gamma\rightarrow\pi}(Q^2)$, including the new BaBar points with $Q^2 = 10 - 40 \text{ GeV}^2$, requires sizeable coefficient a_6 , while a_2 and a_4 remain the same. All-Data-Fit prefers End-Point Enhanced Pion DA.

Conclusions

- By fitting $\pi\gamma$ Transition FF Data in LCSR Approach we obtained Confidential Regions for Gegenbauer coefficients, Moments, and Derivatives of Pion DA.
- Result of fitting the CELLO, CLEO, and BaBar Data up to 9 GeV^2 is in a good agreement with previous CLEO-based fit and prefers the End-Point Suppressed (BMS) Pion DA.
- Taking into account all the data on $F_{\gamma^*\gamma\rightarrow\pi}(Q^2)$, including the new BaBar points with $Q^2 = 10 - 40 \text{ GeV}^2$, requires sizeable coefficient a_6 , while a_2 and a_4 remain the same. All-Data-Fit prefers End-Point Enhanced Pion DA.
- Evident conflict between ($\eta\gamma$ and $\eta'\gamma$) and $\pi^0\gamma$ BaBar Data may signal about strong isospin symmetry violation in pseudoscalar meson sector.

Conclusions

- By fitting $\pi\gamma$ Transition FF Data in LCSR Approach we obtained Confidential Regions for Gegenbauer coefficients, Moments, and Derivatives of Pion DA.
- Result of fitting the CELLO, CLEO, and BaBar Data up to 9 GeV^2 is in a good agreement with previous CLEO-based fit and prefers the End-Point Suppressed (BMS) Pion DA.
- Taking into account all the data on $F_{\gamma^*\gamma\rightarrow\pi}(Q^2)$, including the new BaBar points with $Q^2 = 10 - 40 \text{ GeV}^2$, requires sizeable coefficient a_6 , while a_2 and a_4 remain the same. All-Data-Fit prefers End-Point Enhanced Pion DA.
- Evident conflict between $(\eta\gamma$ and $\eta'\gamma)$ and $\pi^0\gamma$ BaBar Data may signal about strong isospin symmetry violation in pseudoscalar meson sector.
- To resolve BaBar puzzle we need Belle verification of $\pi\gamma$ Transition FF Data.